Pursuit and Saccadic Eye Movement Subregions in Human Frontal Eye Field: A High-resolution fMRI Investigation

Caterina Rosano[1], Christine M. Krisky[4], Joel S. Welling[2], William F. Eddy[2], Beatriz Luna[1], Keith R. Thulborn[3] and John A. Sweeney[1,4]

[1]Neurobehavioral Studies Program, Department of Psychiatry, University of Pittsburgh, Pittsburgh, PA, [2]Department of Statistics, Carnegie Mellon University, Pittsburgh, PA, [3]Department of Radiology and [4]Departments of Psychiatry, Neurology and Psychology, University of Illinois, Chicago, IL, USA

Recent positron emission tomography (PET) and functional magnetic resonance imaging (fMRI) studies in humans have localized the frontal eye field (FEF) to the precentral sulcus (PCS). In macaque monkeys, low-threshold microstimulation and single unit recording studies have located a saccadic subregion of FEF in a restricted area along the anterior wall of the arcuate sulcus and a pursuit subregion located deeper in the sulcus close to the fundus. The functional organization and anatomical location of these two FEF subregions are still to be defined in humans. In the present study, we used fMRI with high spatial resolution image acquisition at 3.0 Tesla to map the saccade- and pursuit-related areas of FEF within the two walls of the PCS in 11 subjects. We localized the saccade-related area to the upper portion of the anterior wall of the precentral sulcus and the pursuit-related area to a deeper region along the anterior wall, extending in some subjects to the fundus or deep posterior wall. These findings localize distinct pursuit and saccadic subregions of FEF in humans and demonstrate a high degree of homology in the organization of these FEF subregions in the human and the macaque monkey.

Introduction

When we explore the visual field, we move our eyes to locate, see and track objects. We use saccadic eye movements to fixate objects of interest that are stable in space and smooth pursuit eye movements to track moving targets. In primates, the frontal eye field (FEF) is a principal neocortical region involved in the execution of both saccadic and pursuit eye movements (Leichnetz and Goldberg, 1988; MacAvoy *et al*., 1991; Gottlieb *et al*., 1993, 1994; Tian and Lynch, 1996b, 1997; Tehovnik *et al*., 2000). This area is located rostral to the central sulcus and in the macaque monkey it has been localized to the arcuate sulcus at the border between Brodmann Areas 8 and 6 (Bruce *et al*., 1985). Intracortical microstimulation (Stanton *et al*., 1989), single-neuron recording (MacAvoy *et al*., 1991; Gottlieb *et al*., 1994) and experimental lesion studies (MacAvoy *et al*., 1991) in non-human primates have also shown that there are separate saccade- and pursuit-related areas within the FEF. In the macaque monkey, neurons in the anterior wall and part of the anterior lip of the arcuate sulcus show task-related changes in activity during saccadic eye movements, while activity of cells in the fundus and deep posterior bank is related to smooth pursuit eye movements.

While the functional anatomy of the monkey FEF has been characterized extensively, much less is known about the functional organization of the FEF in humans. Indeed, earlier human intrasurgical stimulation studies were somewhat inconsistent in their mapping of the human FEF, with Penfield and Rasmussen (Penfield and Rasmussen, 1950) mapping it rostral to the precentral sulcus, but Foerster (Foerster, 1931) mapping it on the rostral lip of the precentral sulcus with small rostral extension.

Functional imaging studies have consistently indicated that in humans the most robust activation during saccadic eye movement tasks lies in an area regarded as Brodmann Area 6, within the superior element of the precentral sulcus (PCS) (Paus, 1996; Luna *et al*., 1998; Courtney *et al*., 1998). This region is now generally accepted to be the site of the human FEF. Thus, in comparison to the monkey FEF, which is located in dysgranular cortex at the border between Brodmann Areas 8 and 6, the human FEF appears to lie entirely in a region believed to be comprised of agranular cortex. This observation raises questions about the homology of the visuomotor system in human and non-human primates.

One approach for assessing the homology of functional organization of human and non-human primate FEF is to determine whether functional principles established for the monkey FEF can be demonstrated in humans. Our aim in this study was to determine whether there is a discrimination of pursuit and saccade regions in FEF along the depth of the precentral sulcus, as has been shown in the arcuate sulcus of the macaque monkey.

Few studies have explored the functional anatomy of the human FEF with regard to the control of pursuit and saccadic eye movements (Petit *et al*., 1997; O'Driscoll *et al*., 1998; Berman *et al*., 1999; Petit and Haxby, 1999; O'Driscoll *et al*., 2000). In general, previous studies have found a high degree of overlap between saccade and pursuit areas. Petit and Haxby (Petit and Haxby, 1999) reported that the mean location across subjects of pursuit-related activation tended to be located deeper than the saccade-related area of activation in the FEF, as is the case in the macaque monkey, but this effect was not seen in similar previous studies. However, precision of mapping in all earlier studies was limited by methodological factors including: (i) low spatial resolution that prohibited discrimination of activation in the anterior and posterior walls of the precentral sulcus and (ii) misregistrations resulting from overlaying T2*-weighted activation maps on T1-weighted anatomic images to localize activations. Further, none of the prior studies in this area considered the high variability of the anatomy of the PCS across individuals, which often includes medial branches in which the potential functional specialization merits investigation. In the present study, we used functional magnetic resonance imaging (fMRI) at 3.0 Tesla with a very high spatial resolution functional imaging method to clarify the functional anatomy of pursuit and saccadic eye movements within the walls and fundus of the PCS.

Materials and Methods

Subjects

Subjects were 11 healthy volunteers recruited from community advertisements. Four were male and seven female and their mean age was 27.2 years (SD = 6.5). Review of medical history revealed no neurologic disease, brain injury, or major psychiatric illness. All subjects but one ambidextrous individual were right-handed. Far visual acuity, corrected or uncorrected, was at least 20/40. Written consent and experimental procedures for this study complied with the Code of Ethics of the World

Medical Association (1964 Declaration of Helsinki) and the Institutional Review Board at the University of Pittsburgh.

Before entering the scanner, subjects spent ~20 min in a mock scanner that simulated the noise and confinement of an actual MR scanner. This was done to habituate them to the MR scanner environment in order to reduce potential anxiety and to stabilize physiological measures such as heart rate and respiration (Rosenberg *et al.*, 1997).

Oculomotor Paradigms

To insure that subjects could perform tasks with a high level of accuracy during the imaging studies, prior evaluation and training were performed as previously described (Luna *et al.*, 1998). Furthermore, immediately before entering the scanner for studies, subjects were retrained on the two simple eye movement tasks. Eye movement activity was not monitored in the scanner, but the previous training and the fact that these simple sensorimotor tasks are performed reflexively and accurately by healthy young subjects make it reasonable to assume that the tasks were, in fact, completed as instructed. Visual stimuli for all paradigms were generated using CIGAL software (Voyvodic, 1996) and projected onto a rear projection screen viewed from an angled mirror fixed to the head coil (Thulborn *et al.*, 1996).

Subjects performed two separate paradigms in the same scan session: (i) smooth pursuit versus central fixation and (ii) visually guided saccades versus central fixation, as described previously (Berman *et al.*, 1999). The order of the two paradigms employed in this block design study was randomly assigned across subjects. Each paradigm used the same baseline condition of central fixation to ensure that the entire large-scale neurocognitive network of activation was mapped for both types of eye movements, including areas of overlap. Blocks of the active eye movement conditions (42 s) alternated with blocks of central fixation (42 s) for 9.5 cycles, starting and ending with the fixation condition. The fixation condition used a white cross-hair subtending 0.75° of visual angle on a dark background. For both eye movement conditions, the target was a white spot subtending 1° of visual angle on a dark background. For the smooth pursuit paradigm, the target moved at an average rate of 10°/s along the horizontal meridian. Motion was sinusoidal across ±10°, a slow speed which healthy human subjects track with few corrective saccades (Dallos and Jones, 1963; Sweeney *et al.*, 1994). For the visually guided saccade paradigm, the target moved every 750 ms in 4° steps to one of five potential locations along the horizontal meridian (0°, ±4° and ±8°). The direction of movement (right or left) was unpredictable except at the ±8° locations from which the target always stepped back toward the center of the screen.

Image Acquisition

All fMRI studies were performed on a 3.0 Tesla scanner (General Electric Medical Systems, Milwaukee, WI) using a commercial quadrature birdcage radiofrequency coil. Subjects' heads were positioned comfortably within the head coil and head motion was minimized with firm cushions. Echo planar imaging (EPI) capabilities were supplied with resonant gradients (Advanced NMR Systems Inc., Wilmington, MA). After performing first-order shimming, functional images were acquired using gradient-echo EPI, which is sensitive to regional alterations in blood flow via blood oxygenation level dependent (BOLD) contrast effects (Kwong *et al.*, 1992). Six axial (horizontal) slices were acquired through the dorsal cerebral cortex to include the superior element of the precentral sulcus (Fig. 1). The following parameters were used for functional scans: TE = 25 ms, flip angle = 90°; segmented partial k-space with oversampling under 'catch and hold' gradients (Thulborn *et al.*, 1997); field of view = 80 × 20 cm; TR = 4.2 s (8.4 s to complete two RF pulses for complete images); 3 mm slice thickness with 1 mm gap. The segmentation of k-space was performed with two separate acquisitions ('two shot') of each half of k-space in the frequency encoding direction to double resolution (Cohen and Weisskoff, 1991). The resonant gradients were modified to lengthen each phase to allow 256 points (instead of 128 points) to be acquired under each lobe of the sinusoidally varying gradient to double the resolution yet again in the frequency encoding direction. The use of partial (56%) k-space acquisition in the phase encoding direction doubled the resolution in this direction. These parameters generated 95 images per slice with voxel dimensions in each image of 0.8 mm anterior to posterior × 1.6 mm left to right × 3.0 mm dorsal to ventral. High-resolution structural images were also acquired in the axial plane [three-dimensional spoiled gradient recalled imaging (SPGR)] with 1.5 mm thick contiguous slices.

Image Analysis

We used locally developed FIASCO software (Functional Imaging Analysis Software – Computational Olio) (Lazar *et al.*, 2001) to de-ghost images and estimate and correct for in-plane head motion in k-space and then to reconstruct images (Eddy *et al.*, 1996). Mean in-plane head displacement was <0.6 mm for both paradigms for each subject.

Task-related activation maps were studied based on the results of

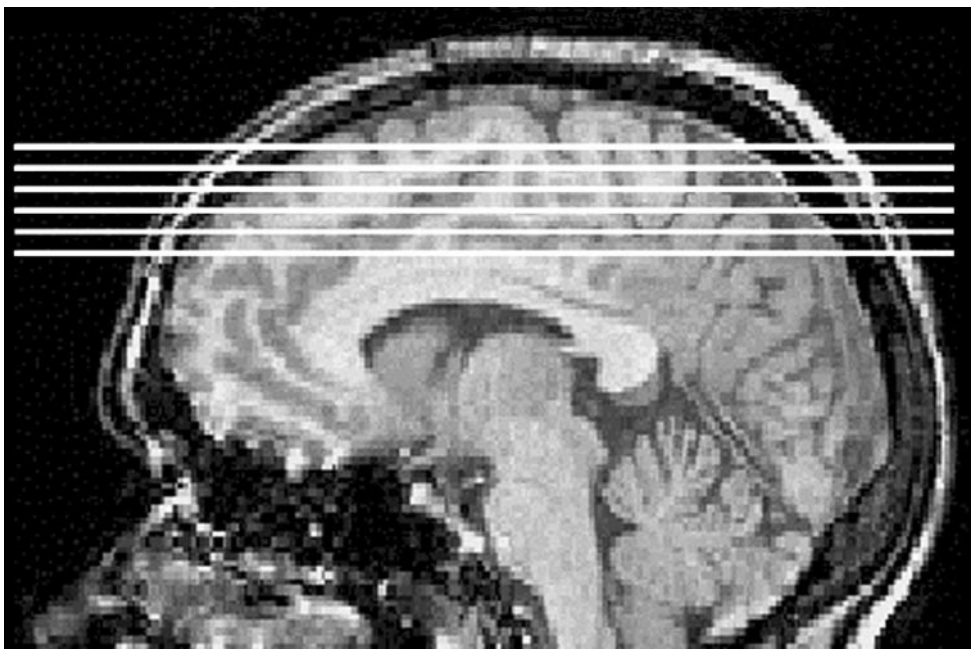

Figure 1. Midsagittal image showing a representative example of the slice prescription used for the imaging protocol. The axial slice prescription that included the superior element of the precentral sulcus is indicated by the horizontal lines.

voxel-wise *t*-tests on data acquired from individual subjects. No spatial filtering was applied in post-processing to the data. The value $t \geq 3.0$ was chosen as a threshold to detect task-related effects. Commonly, fMRI studies use a higher threshold for detecting activation. In this study, our analysis focused only on the relatively small number of voxels constituting the PCS, therefore a lower threshold was used to control Type 1 error rate.

Regions of Interest

Region of interest (ROI) analysis was used to study areas of activation within the PCS. The commonly used approach of superimposing activation maps on T1-weighted structural images was not done to avoid mislocalization of activation in the brain, which results from different image distortions in T1- and T2*-weighted images. Rather, we overlaid the activation map from each subject directly on the middle image in the EPI functional image time series (i.e. the 47th of the 95 images acquired from each slice) to localize activation effects. This strategy was made possible by the high spatial resolution of our functional images, which permitted visualization of regions of interest in the functional images themselves (Fig. 2*A*,*B*).

For each subject and each task, regions of interest were drawn manually on the selected functional image, guided by concurrent viewing of the SPGR anatomic images, but without knowledge of activation maps. This was achieved using AFNI software (Cox, 1996), which provided simultaneous viewing of sagittal, coronal and horizontal planes of both SPGR and functional images. The atlas of Duvernoy (Duvernoy *et al*., 1991) was used for consultation. ROIs were drawn to include all gray matter comprising sulci of interest. Examination of the SPGR images and the fMRI time series (Lee *et al*., 1995) was used to identify large draining veins proximal to regions of interest, and these areas were excluded from ROIs.

We found that there were certain relatively common characteristics of the anatomy of the PCS that we wanted to take into account in our definitions of regions of interest. As illustrated by Ono *et al*. (Ono *et al*., 1990), the PCS commonly has side branches at its most medial extent. We defined medial branches of the PCS as those sulci extending for >1 cm from the main body of the PCS and running toward the midline in the rostral direction (antero-medial branch, AB, see Fig. 2*C*) and in the caudal direction (postero-medial branch, PB, see Fig. 2*C*). Eight of our subjects had this bifurcation pattern bilaterally and the other three showed it in one hemisphere. Due to the consistent presence of these medial branches across subjects and their ambiguous relationship with the main body of the PCS, we examined activation in these branching sulci separately.

We defined six regions of interest in the axial plane (see Fig. 2*C*). Two were the anterior and posterior walls of the main body of the PCS, while the other four were the anterior and posterior walls of the antero-medial branch and of the postero-medial branch of the PCS, respectively. To define boundaries of sulci at points of sulcal intersection, we used the point where there was a gap between the sulci – often evident in images of deeper aspects of sulci because sulci often are shallow at points of sulcal junction – to determine the limits of sulci of interest as suggested by Ono *et al*. (Ono *et al*., 1990). This procedure was of particular importance for distinguishing the borders between the antero-medial branch of the PCS and the posterior-most aspect of the superior frontal sulcus, which not uncommonly intersect (Ono *et al*., 1990).

Image Normalization

Due to high variability in sulcal localization, shape and size across individuals, comparison of the anatomical distribution of activation in the PCS across subjects required a procedure that would rescale images from

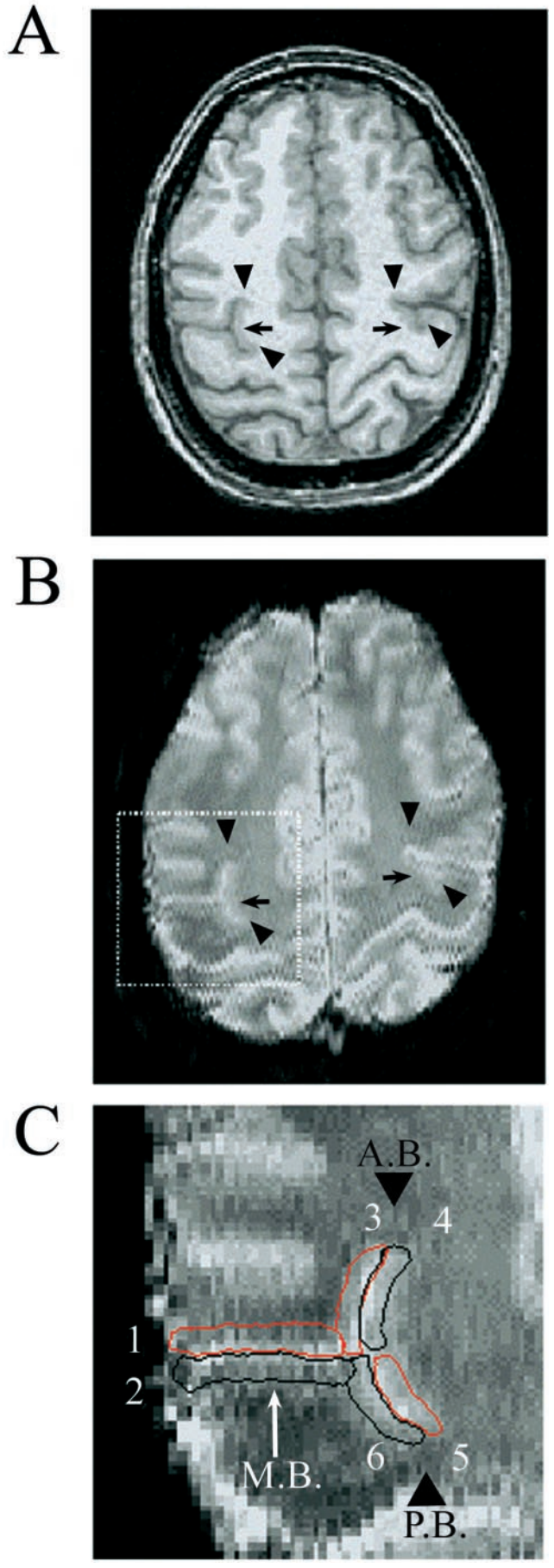

Figure 2. Axial T1-weighted (SPGR) (*A*) and T2*-weighted (*B*) two shot catch and hold images of one subject showing the high correspondence of the anatomical structures of interest in the two types of images. Arrows indicate the corresponding precentral sulcus in these images. Arrowheads point to the medial branches of the precentral sulcus (A.B., antero-medial branch; P.B., postero-medial branch). (*C*) Detail of the highlighted section in (*B*), indicating the six regions of interest drawn on this subject's image. The regions drawn in red indicate the anterior walls; black is for posterior wall. Arrowheads point to the antero-medial and postero-medial branches of the precentral sulcus (A.B. and P.B., respectively). The white arrow indicates the main body of the PCS (M.B.). The six ROIs are numbered from 1 to 6 and are referred to in this way in the text.

each individual subject to a common metric in order to allow averaging of results across subjects. In each of the three sulci of interest, we aligned and rescaled activation maps relative to their depth from the cortical surface to the fundus along the *z*-coordinate axis (dorsal to ventral) using the following procedure: (i) the SPGR slices containing the deepest and the most dorsal points of the sulcus (fundus and dorsum, respectively) were identified; (ii) the SPGR slice number including the fundus was set equal to zero, the SPGR slice including the dorsum to 100 and slices between these images were set to their proportional distance between the two reference images in order that the location of slices could be considered in terms of their percentage distance from the fundus to the cortical surface (see Fig. 3); (iii) the middle functional image set in the fMRI time series from each subject was aligned with their SPGR anatomical image set to locate the depth of each functional image relative to sulcal depth of each ROI in each hemisphere; and (iv) we rescaled the *z*-coordinate values of the functional slices according to the same 0–100 coordinate system as used for the SPGR anatomic images. Therefore, the depth of each functional slice was expressed as a percentage of its distance from the fundus to the cortical surface in each ROI. For each subject, each unit percentage of this portion was assigned the value of activation carried by its corresponding functional slice.

Using this method, we localized and quantified activation in the ROIs of each subject without the use of the Talairach system. If we had averaged effects across subjects in Talairach proportional space, we would have lost necessary spatial resolution needed to distinguish effects in the anterior and posterior walls of the PCS.

Data Analysis

We computed the total number of voxels and the number of voxels showing significant task-related activation for each ROI. For each subject and for each task, activation in each ROI was computed as the percentage of voxels in that ROI showing task-related activity (number of active voxels with significant activation/number of voxels in ROI) to allow comparisons of activity in ROIs across subjects. To analyse the distribution of activation along the depth of the sulcus, the percentage of voxels showing task-related activation was also computed for each slice. For each subject and each ROI, we also determined the region with the largest proportion of activated voxels for each task and identified its depth along the sulcal wall (percentage depth of the center of the functional slice).

Results

Execution of both pursuit and saccadic eye movements was associated with bilateral activation in the precentral gyrus and in its medial branches. The pattern of activation during both tasks is shown in Fig. 4 for one representative subject. This figure illustrates that during the saccade task the activation was mostly localized in the portion of the PCS close to the cortical surface (slice numbers 1–3), while during the pursuit task the activation was most robust in a deeper portion of the PCS close to the fundus.

Analysis of Task-related Activation in Each ROI

The spatial extent of activation (calculated here as the percentage of each ROI's area) during the saccade task was significantly greater than that of pursuit-related activity (Fig. 5). This was true in both the main body of the precentral sulcus and in its medial branches in both the right [PCS, $t(10) = 2.6$, $P < 0.05$; antero-medial branch, $t(9) = 3.3$, $P < 0.01$; postero-medial branch, $t(9) = 2.7$, $P < 0.05$] and left hemispheres [PCS, $t(10) = 2.5$, $P < 0.05$; antero-medial branch, $t(10) = 2.2$, $P < 0.05$; postero-medial branch, $t(9) = 3.0$, $P < 0.05$].

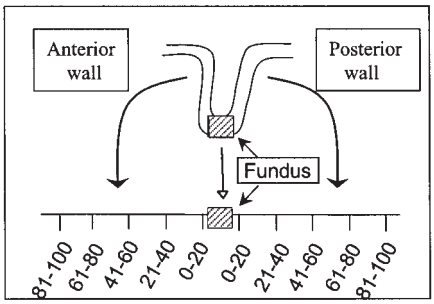

Figure 3. Diagram showing the strategy used to normalize measurements of activation in the precentral sulcus. The dashed box indicates the location of the fundus of the sulcus before and after the normalization procedure. See text for details.

The extent of activation in the anterior and posterior walls of the sulci of interest during each eye movement task is illustrated in Figure 6. In the main body of the PCS, for both hemispheres, the extent of saccade-related activation in the anterior wall was significantly higher than in the posterior wall [right, $t(10) = 3.6$, $P < 0.005$; left, $t(10) = 2.3$, $P < 0.05$]. Activation in the anterior wall of the PCS was also greater than in the posterior wall during the pursuit task in both hemispheres [right, $t(10) = 2.2$, $P < 0.05$; left, $t(10) = 2.5$, $P < 0.04$]. We did not find any statistically significant difference in the extent of activation between the two walls in the antero- or postero-medial branches of the PCS in either task in either hemisphere.

Hemispheric Effects

We found no significant hemispheric difference in the extent of activation during either the saccade or pursuit tasks in any sulcus of interest (Fig. 5). Further analysis revealed no laterality effects during either task when examining effects in each sulcal wall in each region of interest separately (Fig. 6).

Distribution of Activation along the Depth of Sulci

We examined the distribution of active voxels as a function of their depth along the sulci of interest – from the dorsum to the fundus – during each eye movement task. Figure 7*A* shows that in the right hemisphere during the saccade task, most of the active voxels (61 ± 12% of the total number of active voxels in the entire PCS) were localized in the upper portion of the anterior wall of the PCS, i.e. from 40 to 100% of the distance above the fundus. In contrast, during the pursuit task most of the active voxels (64 ± 11% of the total number of active voxels in the entire PCS) were segregated close to the fundus of the PCS, <40% of the distance above the fundus along the two walls. Statistical comparison showed that the extent of pursuit-related activity was significantly greater than saccade-related activation at 20–40% away from the fundus along the posterior wall [$t(10) = 2.8$, $P < 0.05$], while the extent of saccade-related activity was significantly greater than pursuit-related activity along a region of the anterior wall extending from 40 to 100% of the distance above the fundus [at 80–100%, $t(10) = 4.6$, $P < 0.005$; at 60–80%, $t(10) = 4.5$, $P < 0.005$; at 40–60%, $t(10) = 3.1$, $P < 0.05$].

In the left hemisphere, 50 ± 10% of the total number of active voxels during the saccade task clustered at 40–100% of the distance above the fundus in the anterior wall, and the extent of

Figure 4. Activation during smooth pursuit and visually guided saccades each compared to visual fixation shown for one individual subject in the right and left hemisphere (R and L, respectively). The left column shows the six functional slices acquired; the insets enclosed in the dashed box for each slice are illustrated in the right column at a higher magnification. Red indicates activation during pursuit, blue indicates activation during saccades and yellow indicates activation observed during both tasks. Only activation effects in voxels with *t* value >3.0 are shown in color.

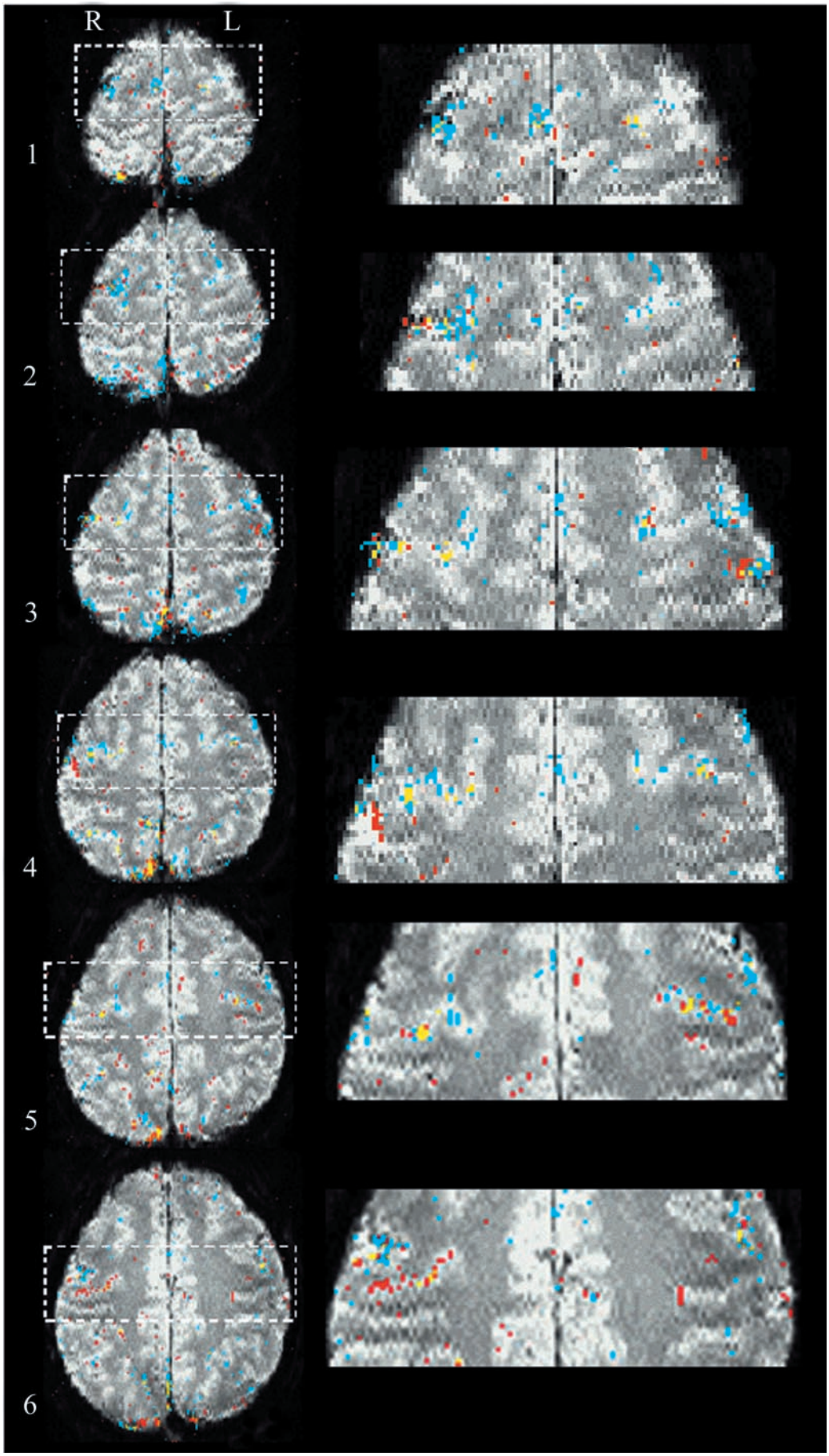

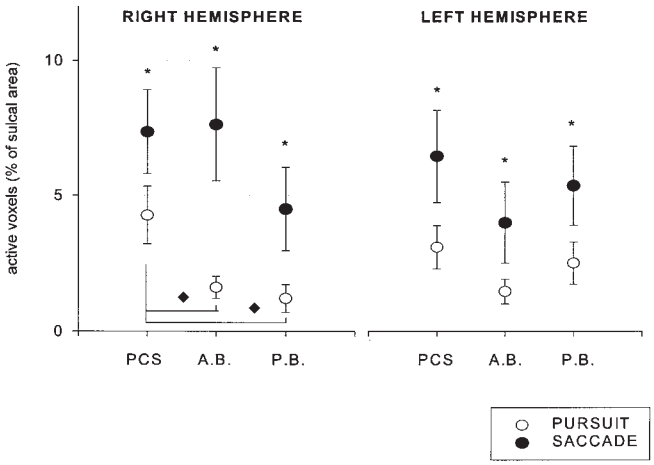

Figure 5. Spatial extent of activation during saccade and pursuit tasks in the precentral sulcus (PCS) and in its antero-medial and postero-medial branches (A.B. and PB., respectively). Average across subjects ± SEM are shown separately for the right and the left hemisphere. Asterisks indicate significant differences in activation observed between the saccade and pursuit tasks in the three sulci of interest. Diamond symbols (◆) indicate significant differences between spatial extent of pursuit-related activation between the precentral sulcus and its medial branches. * and ◆, $P < 0.05$.

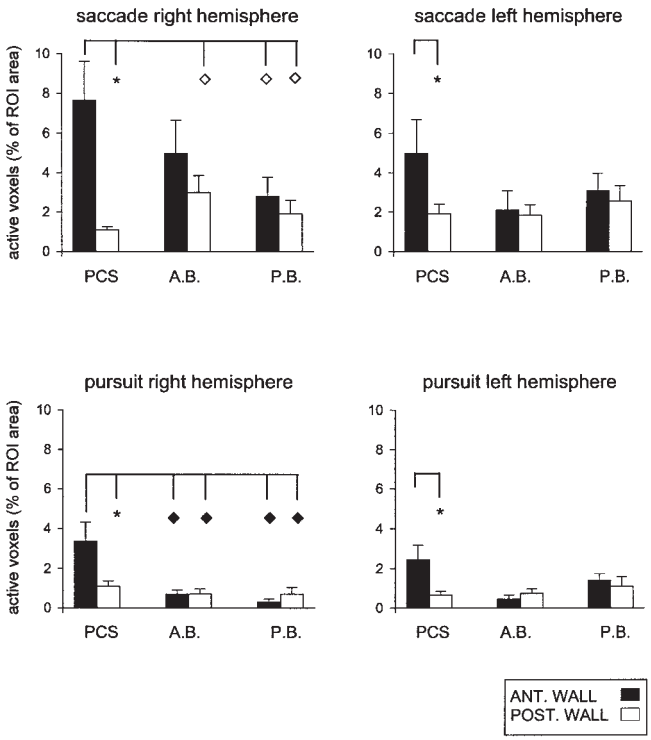

Figure 6. Spatial extent of activation in the anterior (black) and posterior wall (white) of the sulci are illustrated as the average across subjects ± SEM. Results are shown separately for the right (right column) and left hemisphere (left column) and for saccade (top histograms) and pursuit task (bottom histograms). Asterisks indicate significant task-related differences observed in the two walls of the precentral sulcus (PCS). White diamond symbols (◇) indicate significant differences between spatial extent of saccade-related activation between the precentral sulcus-anterior wall and the walls of its medial branches. Black diamond symbols (◆) indicate significant differences between spatial extent of pursuit-related activation between the precentral sulcus-anterior wall and each of the walls of its medial branches. *, ◇ and ◆, $P < 0.05$.

saccade-related activity was significantly greater than pursuit-related activity at 80–100% of the distance above the fundus [$t(10) = 2.8$, $P < 0.05$] as shown in Figure 7*B*. We did not observe any anatomical segregation of the pursuit-related activity along sulcal walls of the left PCS, where pursuit-related activation was modest.

Interestingly, in the right hemisphere, the antero-medial branch showed the same pattern of saccade- and pursuit-related activation as was observed in the main body of the PCS (Fig. 7*C*). We found that 48 ± 24% of the total number of active voxels during the saccade task segregated at 40–100% of the distance above the fundus in the anterior wall and at this location the extent of saccade-related activity was significantly greater than that of pursuit [at 80–100%, $t(10) = 2.8$, $P < 0.05$; at 60–80%, $t(10) = 2.6$, $P < 0.05$; at 40–60%, $t(10) = 2.7$, $P < 0.05$]. During the pursuit task, 49 ± 11% of the active voxels were located close to the fundus in a region which extended from 20% of the distance above the fundus along the anterior wall up to 40% of the distance above the fundus along the posterior wall. We did not observe any anatomical segregation of pursuit and saccade regions in the postero-medial branch in the right hemisphere or in either medial branch of the PCS in the left hemisphere.

Location of Peak Activation: Individual Subject Analysis

After measuring the extent of activation separately in each wall in each slice, analysis of individual subject data showed that in the right hemisphere, the region of the main body of the PCS with the highest proportion of active voxels during the saccade task was located in the anterior wall for all subjects. Further, the peak location of the pursuit-related task was consistently inferior to the saccade-related peak location on the anterior wall, or on the posterior wall, in all subjects. This consistent difference in location of peak activation across tasks was statistically significant [$t(10) = 3.7$, $P < 0.005$; Fig. 8*A*]. In all but two subjects (S_1, S_5), the peak location of saccade-related activation was located in the upper half of the anterior wall of the PCS. In all but one subject (S_2), the peak location of pursuit-related activation was in the lower half of the anterior wall or along the posterior wall. In the left hemisphere, the difference between the peak locations across tasks was also statistically significant [$t(10) = 2.9$, $P < 0.05$] and in all but one subject, the peak location of pursuit-related activity was inferior to the peak location of saccade-related activity (S_4).

Comparison of Patterns of Activation Across Different ROIs

The contribution to saccade-related activity was similar in the three regions of interest in both the right and left hemispheres. As it is shown in Figure 5, we did not observe any statistically significant difference in spatial extent of saccade-related activation between the main body of the PCS and its two medial branches in either hemisphere. In the right hemisphere, the extent of pursuit-related activity in the PCS was significantly greater than in either of its medial branches [PCS versus AB, $t(9) = 2.3$, $P < 0.05$; PCS versus PB, $t(9) = 2.7$, $P < 0.05$], indicating that the region contributing to the control of smooth pursuit eye movement was preferentially located in the main body of the PCS. In the left hemisphere, there were no significant differences in the extent of pursuit-related activation between the main body of the PCS and its medial branches.

The anterior versus posterior wall analysis illustrated in Figure 6 demonstrated that in both hemispheres the extent of activation in the PCS anterior wall during the saccade task was greater than in any other ROIs, suggesting that the region contributing to the control of visually guided saccades was preferentially located in

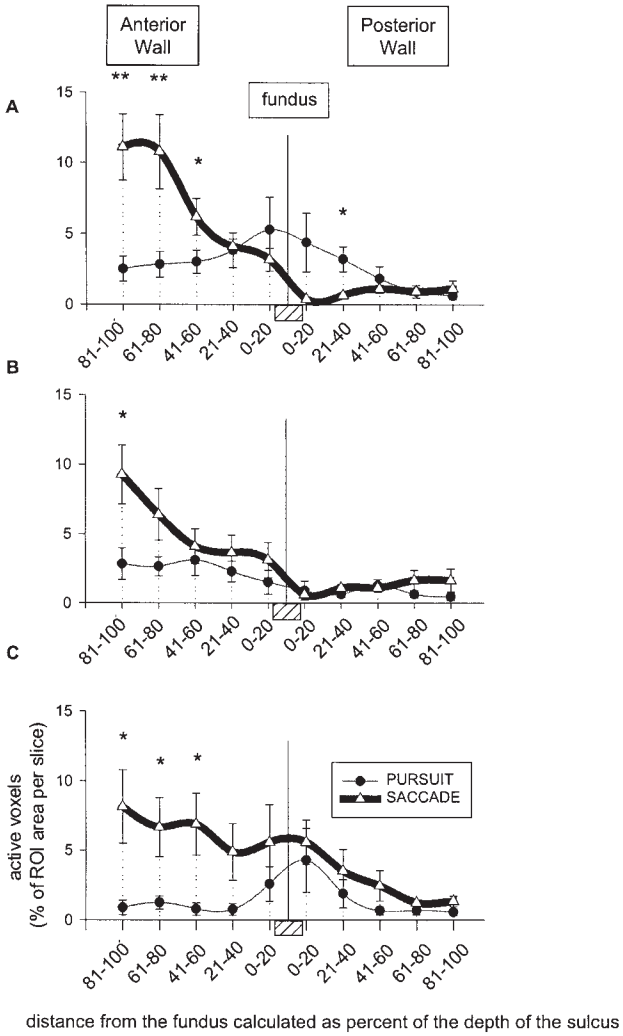

Figure 7. Gradients of activation in the anterior and posterior wall of right precentral sulcus (*A*), left precentral sulcus (*B*) and right antero-medial branch (*C*) are illustrated as the average across subjects ± SEM. The amount of activation is shown here along the depth of the sulcus as described in the Materials and Methods and Figure 3. Asterisks indicate significant differences between the spatial extent of activation between the saccade and pursuit tasks observed at the same location along the walls of the sulcus. $^{*}P < 0.05$, $^{**}P < 0.005$.

the anterior wall of the PCS. This difference reached statistical significance in the right hemisphere for all of the ROIs except the anterior wall of the antero-medial branch (see Fig. 6). Similarly, in the right hemisphere, the pursuit task elicited an area of activation that was significantly greater in the anterior wall of the PCS than in any other ROI (see Fig. 6). This pattern was similar but not significant in the left hemisphere, where only differences between the anterior and posterior walls of the main body of the PCS were significant.

Discussion

The findings of the present study advance understanding of the human FEF in several ways. First, they provide the first evidence localizing the FEF to the anterior wall and fundus of the precentral sulcus. Second, they suggest an important role for the control of eye movements for the medial branches of the PCS in addition to its main body. Third, they indicate a homologous organization of the FEF in the human precentral sulcus and the macaque arcuate sulcus for the control of saccadic and pursuit eye movements. In both species, the saccade-related area is dorsal to the pursuit-related area in the sulcus containing the FEF. All of our subjects showed the highest proportion of activated voxels in the PCS anterior wall during the saccade task, while the highest proportion of the pursuit-related active voxels was located close to the fundus of the PCS, either deeper along the anterior wall or on the posterior wall of the PCS. This pattern was consistent among subjects in our sample and was confirmed in the across-subject averages.

Our data extend and add substantial new information to our knowledge of the human FEF provided by previous functional imaging studies (O'Driscoll *et al.*, 1998; Berman *et al.*, 1999; Petit and Haxby, 1999), which did not consistently differentiate saccade and pursuit subregions within the human FEF. It is likely that the source for these contradictory findings originate from methodological issues regarding spatial resolution and accuracy of spatial localization of activation effects. The spatial resolution used in previous studies did not allow for a discrimination of activation in the two walls of the PCS, so that activation in the anterior and posterior walls could not be distinguished. The consequences of this are clear when examining the location of pursuit- and saccade-related peak activation in four of our subjects (S_3, S_4, S_6 and S_9) as illustrated in Figure 8*A*. If the PCS of these subjects was seen as a single structure rather than composed of two walls, the distance between pursuit and saccade areas – here located at a similar depth in the sulcus – could be greatly underestimated and the two regions could be considered overlapping. For this reason, in the present study, we investigated the location of task-related activation in individual subjects relative to their specific sulcal anatomy. Indeed, our high- resolution imaging method allowed us to address the spatial organization of saccade- and pursuit-related functions with a spatial precision comparable to that available when unit recording data are used to map functional cortical regions.

Pattern of Activation in the Medial Branches

Our strategy of individual subject analysis not only accounted for inter-subject variability in the gross anatomy of the PCS along both walls of sulci of interest, but also allowed us to characterize task-related activation in the medial branches of the PCS. We separately studied the pattern of activation of these medial branches of the PCS because, despite the high frequency of their incidence (Ono *et al.*, 1990), their functional relationship with the PCS and other adjacent sulci, such as the superior frontal sulcus, was unclear. While the boundary between the PCS and the most caudal portion of the superior frontal sulcus has been shown to be active during oculomotor tasks, its functional specialization for spatial working memory is still debated (Courtney *et al.*, 1998; Postle *et al.*, 2000). We found that both medial branches of the PCS had generally similar patterns of task-related activation as observed in the main body of the PCS. Further, the saccade-related activity found in the dorsal portion of the anterior wall of both the PCS and its antero-medial branch, as contrasted to the pursuit-related activity localized closer to the fundus in both of these regions, indicates a high functional homology between these two structures. This high similarity, together with the anatomical relationship of the main body of the PCS and its antero-medial branch (see Fig. 2), suggests that the antero-medial branch of the PCS may include a portion of the FEF.

A question might be raised as to whether the region we identified as the antero-medial branch of the PCS was actually the most posterior aspect of the superior frontal sulcus. Based on

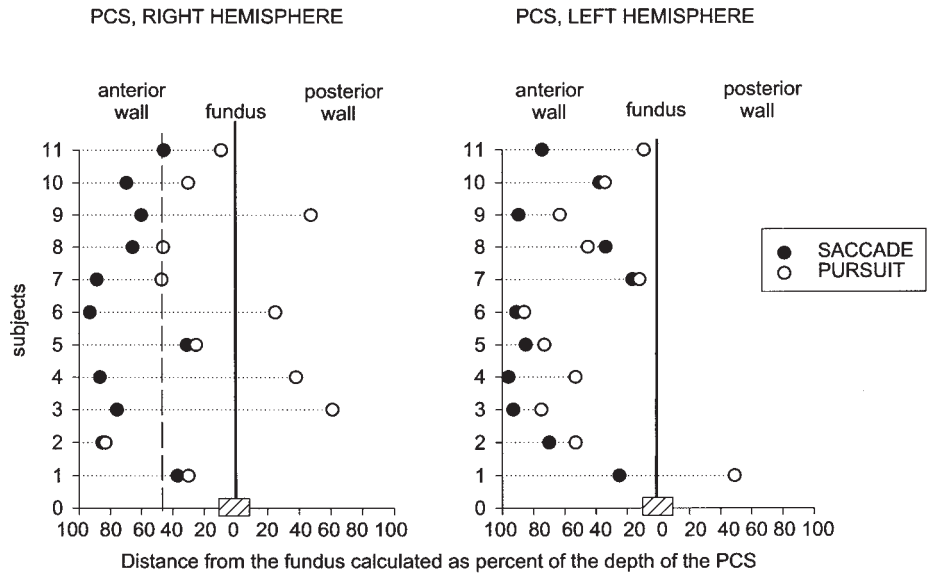

Figure 8. Location of peak activation for each individual subject during the saccade (black) and pursuit tasks (white). Results are shown separately for the right and left precentral sulcus (PCS). The saccade-related peak of activation was always located in the upper portion of the anterior wall, while the location of the pursuit-related peak activation was typically closer to the fundus of the sulcus, or in the posterior wall.

several considerations discussed below, we believe that we in fact observed activation in the antero-medial branch of the PCS and not in the superior frontal sulcus. First, we outlined the ROIs in each individual subject, after the adjacent sulci were studied in the anatomical images. Second, a junction between the superior frontal sulcus and the antero-medial branch was observed in one hemisphere in six of our subjects and only one of these (S_{10}) showed some modest saccade-related activation rostral to the PCS antero-medial branch. Third, we never observed any robust extension of activation beyond the most rostral extent of the PCS antero-medial branch during either of the two tasks in any of the other subjects.

Hemispheric Differences

Overall, activation patterns were generally similar in the left and right hemispheres, although some hemispheric differences were observed. The pattern of pursuit-related activation found in the fundus of the PCS in the right hemisphere was not confirmed in the left and therefore we could not locate a left FEF region specialized for pursuit. Further, we could not anatomically differentiate discrete regions of saccade- and pursuit-related activation in the antero-medial branch of the left PCS as we did in the right hemisphere. The dominant role of the right hemisphere for redirecting attention during visuospatial tasks is well documented (Mesulam, 1981) and may account for the somewhat greater activation observed in the right hemisphere during our oculomotor tasks. Such an attentional enhancement may have increased the gain of task-related activation and thereby allowed a successful discrimination of pursuit- and saccade-related activation in more regions of interest and over larger extents of tissue within ROI in the right hemisphere.

Similarly, the finding that the FEF seems to be more active during saccades than pursuit (Petit *et al.*, 1997; Berman *et al.*, 1999; O'Driscoll *et al.*, 2000) could explain why we could localize a cluster of saccade-related activity in both hemispheres, while we only found a right but not a left hemisphere pursuit-related area of activation. The less robust activation during pursuit tasks might have contributed to our inability to detect a gradient of pursuit-related activation in the left hemisphere. In this regard, it is important to note that the high spatial resolution provided by our fMRI method and the use of individual subject data rather than group average activation maps may have been disadvantageous in terms of sensitivity to blood oxygenation level dependent (BOLD) activation effects. This could be another factor accounting for why we could not differentiate pursuit and saccade areas along the walls of the left FEF. It is unlikely, in our view, that a pursuit-related area does not exist in the left hemisphere, because clinical studies have shown that lesions in each of the two hemispheres disrupt ipsilateral pursuit (Rivaud *et al.*, 1994; Morrow and Sharpe, 1995).

Conclusions

Our findings indicate that the organization of saccade- and pursuit-related areas within the human PCS is homologous to the functional organization of oculomotor areas that have been delineated in the FEF of macaque monkey, in which saccade and pursuit regions have been located in the anterior bank and fundus of the arcuate sulcus respectively (Bruce *et al.*, 1985; MacAvoy *et al.*, 1991; Gottlieb *et al.*, 1993; Tian and Lynch, 1996a). However, the fact that in the macaque monkey the FEF region is located at the border between granular and agranular cortex, while the PCS in humans is located in an area believed to be comprised of agranular cortex, appears to place the monkey FEF in a more rostral location than the human FEF. Courtney *et al.* (Courtney *et al.*, 1998) advanced the hypothesis that the philogenetical development of the human brain may have caused the FEF to move posteriorly and superiorly to devote more functional capacity to new specialized functions such as language. Another possibility is that in humans, the border between Brodmann Areas 6 and 8 – and thus the posterior-most aspect of granular/dysgranular cortex – is more posterior than was appreciated in classic cytoarchitectural mapping studies. If this were the case, the human FEF could be in a region cytoarchitectonically homologous to the monkey FEF. Detailed studies of the cytoarchitecture, myeloarchitecture and patterns of efferent and afferent connectivity of the human PCS using

methods of post-mortem tracing (Mesulam, 1979; Dai *et al.*, 1998; Clarke *et al.*, 1999; Di Virgilio *et al.*, 1999), integrated with findings from *in-vivo* functional imaging investigations using different approaches such as linking brain activation with eye movement and eye blink activity on a trial-wise basis, are needed conclusively to confirm the homology between human and monkey in the anatomical organization of these two functionally defined areas.

Notes

This work was supported by the NIH (NS33355, HD35469, MH01433, MH42969, MH45156, MH62134) and NARSAD. We gratefully acknowledge the assistance of Rebecca Berman, Tomika Cohen, Christopher Genovese, Nicole Lazar and Kimberly Skinner for helpful comments throughout the planning and implementation of this investigation.

Address correspondence to John A. Sweeney, Department of Psychiatry, University of Illinois – Chicago, 912 S. Wood St, M/C 913, Chicago, IL 60612, USA. Email: jsweeney@psych.uic.edu.

References

Berman RA, Colby CL, Genovese CR, Voyvodic JT, Luna B, Thulborn KR, Sweeney JA (1999) Cortical networks subserving pursuit and saccadic eye movements in humans: an fMRI study. Hum Brain Mapp 8: 209–225.

Bruce CJ, Goldberg ME, Bushnell MC, Stanton GB (1985) Primate frontal eye fields. II. Physiological and anatomical correlates of electrically evoked eye movements. J Neurophysiol 54:714–734.

Clarke S, Riahi-Arya S, Tardif E, Eskenasy AC, Probst A (1999) Thalamic projections of the fusiform gyrus in man. Eur J Neurosci 11: 1835–1838.

Cohen MS, Weisskoff RM (1991) Ultra-fast imaging. Magn Reson Imaging 9:1–37.

Courtney SM, Petit L, Maisog JM, Ungerleider LG, Haxby JV (1998) An area specialized for spatial working memory in human frontal cortex. Science 279:1347–1351.

Cox RW (1996) AFNI: software for analysis and visualization of functional magnetic resonance neuroimages. Comput Biomed Res 29:162–173.

Dai J, Swaab DJ, Van Der Vliet J, Buijs RM (1998) Postmortem tracing reveals the organization of hypothalamic projections of the suprachiasmatic nucleus in the human brain. J Comp Neurol 400:87–102.

Dallos PJ, Jones RW (1963) Learning behavior of the eye-fixation control system. IEEE Trans Autom Contr 8:218–227.

Di Virgilio G, Clarke S, Pizzolato G, Schaffner T (1999) Cortical regions contributing to the anterior commissure in man. Exp Brain Res 124: 1–7.

Duvernoy H, Cabanis EA, Iba-Zizen MT, Tamraz J, Guyot J (1991) The human brain. New York: Springer.

Eddy WF, Fitzgerald M, Noll DC (1996) Improved image registration by using Fourier interpolation. Magn Res Med 36:923–931.

Foerster O (1931) The cerebral cortex in man. Lancet 2:309–312.

Gottlieb JP, Bruce CJ, MacAvoy MG (1993) Smooth eye movements elicited by microstimulation in the primate frontal eye field. J Neurophysiol 69:786–799.

Gottlieb JP, MacAvoy MG, Bruce CJ (1994) Neural responses related to smooth-pursuit eye movements and their correspondence with electrically elicited smooth eye movements in the primate frontal eye field. J Neurophysiol 72:1634–1653.

Kwong KK, Belliveau JW, Chesler DA, Goldberg IE, Weisskoff RM, Poncelet BP, Kennedy DN, Hoppel BE, Cohen MS, Turner R, (1992) Dynamic magnetic resonance imaging of human brain activity during primary sensory stimulation. Proc Natl Acad Sci USA 89:5675–5679.

Lazar N, Genovese CR, Eddy WF, Welling J (2001) Statistical issues in fMRI for brain imaging. Int Statist Rev 69:105–127.

Lee AT, Glover GH, Meyer CH (1995) Discrimination of large venous vessels in time-course spiral blood-oxygen-level-dependent magnetic resonance functional neuroimaging. Magn Reson Med 33:745–754.

Leichnetz GR, Goldberg ME (1988) Higher centers concerned with eye movement and visual attention: cerebral cortex and thalamus. Rev Oculomot Res 2:365–429.

Luna B, Thulborn KR, Strojwas MH, McCurtain BJ, Berman RA, Genovese CR, Sweeney JA (1998) Dorsal cortical regions subserving visually-guided saccades in humans: an fMRI study. Cereb Cortex 8:40–47.

MacAvoy MG, Gottlieb JP, Bruce CJ (1991) Smooth pursuit eye movement representation in the primate frontal eye field. Cereb Cortex 1:95–102.

Mesulam MM (1979) Tracing neuronal connections of human brain with selective silver impregnation. Observations on geniculocalcarine, spinothalamic and entorhinal pathways. Arch Neurol 36:814–818.

Mesulam MM (1981) A cortical network for directed attention and unilateral neglect. Ann Neurol 10:309–325.

Morrow MJ, Sharpe JA (1995) Deficits of smooth-pursuit eye movement after unilateral frontal lobe lesions. Ann Neurol 37:443–451.

O'Driscoll GA, Strakowski SM, Alpert NM, Matthysse SW, Rauch SL, Levy DL, Holzman PS (1998) Differences in cerebral activation during smooth pursuit and saccadic eye movements using positron emission tomography. Biol Psychiatry 44:685–689.

O'Driscoll GA, Wolff AV, Benkelfat C, Florencio PS, Lal S, Evans AC (2000) Functional neuroanatomy of smooth pursuit and predictive saccades. NeuroReport 11:1335–1340.

Ono M, Kubik S, Abernathy CD (1990) Atlas of the cerebral sulci. New York: Thieme Medical.

Paus T (1996) Location and function of the human frontal eye-field: a selective review. Neuropsychologia 34:475–483.

Penfield W, Rasmussen T (1950) The cerebral cortex of man. A clinical study of localization of function. New York: MacMillan.

Petit L, Haxby J (1999) Functional anatomy of pursuit eye movements in humans as revealed by fMRI. J Neurophysiol 82:463–471.

Petit L, Clark VP, Ingeholm J, Haxby JV (1997) Dissociation of saccade-related and pursuit-related activation in human frontal eye fields as revealed by fMRI. J Neurophysiol 77:3386–3390.

Postle B, Berger J, Taich A, D'Esposito M, (2000) Activity in human frontal cortex associated with spatial working memory and saccadic behavior. J Cogn Neurosci 12(Suppl. 2):2–14.

Rivaud S, Muri RM, Gaymard B, Vermersch AI, Pierrot-Deseilligny C (1994) Eye movement disorders after frontal eye field lesions in humans. Exp Brain Res 102:110–120.

Rosenberg DR, Sweeney JA, Gillen J, Kim J, Varenelli M, O'Hearn K, Erb P, Davis D, Thulborn K (1997) Magnetic resonance imaging of children without sedation: preparation with simulation. J Am Acad Child Adolesc Psychiatry 36:853–859.

Stanton GB, Deng SY, Goldberg ME, McMullen NT (1989) Cyto-architectural characteristic of the frontal eye fields in macaque monkeys. J Comp Neurol 282:415–427.

Sweeney JA, Clementz BA, Haas GL, Escobar MD, Drake K, Frances AJ (1994) Eye tracking dysfunction in schizophrenia: characterization of component eye movement abnormalities, diagnostic specificity, and the role of attention. J Abnorm Psychol 103:222–230.

Tehovnik EJ, Sommer MA, Chou IH, Slocum WM, Schiller PH (2000) Eye fields in the frontal lobes of primates. Brain Res Rev 32:413–448.

Thulborn KR, Davis D, Erb P, Strojwas M, Sweeney JA (1996) Clinical fMRI: implementation and experience. NeuroImage 4:101–107.

Thulborn KR, Chang SY, Shen GX, Voyvodic JT (1997) High resolution echo-planar fMRI of human visual cortex at 3.0 Tesla. NMR Biomed 10:183–190.

Tian JR, Lynch JC (1996a) Functionally defined smooth and saccadic eye movement subregions in the frontal eye field of cebus monkeys. J Neurophysiol 76:2740–2753.

Tian JR, Lynch JC (1996b) Corticocortical input to the smooth and saccadic eye movement subregions of the frontal eye field in cebus monkeys. J Neurophysiol 76:2754–2771.

Tian JR, Lynch JC (1997) Subcortical input to the smooth and saccadic eye movement subregions of the frontal eye field in cebus monkey. J Neurosci 17:9233–9247.

Voyvodic JT (1996) Real-time fMRI paradigm control software for integrating stimulus presentation, behavioral and physiological monitoring, and statistical analysis. Proc Int Soc Magn Reson Med 3:1835.